doi.org/10.26434/chemrxiv.7851461.v2

Proton Conductive Membranes Based on Carboxylated Cellulose Nanofibres and Their Proton Exchange Membrane Fuel Cell Performance

Valentina Guccini, Annika Carlson, Shun Yu, Göran Lindbergh, Rakel Wreland Lindström, Germán Salazar-Alvarez

Submitted date: 18/03/2019 • Posted date: 18/03/2019

Citation information: Guccini, Valentina; Carlson, Annika; Yu, Shun; Lindbergh, Göran; Wreland Lindström, Rakel; Salazar-Alvarez, Germán (2019): Proton Conductive Membranes Based on Carboxylated Cellulose Nanofibres and Their Proton Exchange Membrane Fuel Cell Performance. ChemRxiv. Preprint.

The performance of carboxylated cellulose nanofibers (CNF) membranes has been measured in-situ as a function of CNF surface charge (600 and 1550 µmol g-1), membrane thickness and fuel cell relative humidity (RH 55 to 95 %). The structural evolution of the membrane as a function of RH has been measured by Small Angle X-ray scattering, showing that water channels are formed above 75 % RH. The amount of absorbed water depends on the membrane surface charge and counter ions (Na+ or H+). The high affinity of CNF for water and the high aspect ratio of the nanofibers, together with a well-defined and homogenous membrane structure, ensures a proton conductivity exciding 1 mS cm-1 at 30 °C between 65 and 95 % RH, around two orders of magnitude larger than previously reported values and only one order of magnitude lower than Nafion 212. Moreover, the CNF membranes are characterized by a lower hydrogen crossover than Nafion, despise been ≈ 30 % thinner. Thanks to their environmental compatibility and promising fuel cell performance the CNF membranes should be considered for new generation PEMFCs.

File list (2)

Supporting Information

Proton conductive membranes based on carboxylated cellulose nanofibres and their proton exchange membrane fuel cell performance

Valentina Guccini[†,§,‡], Annika Carlson[‖,‡], Shun Yu[†,§,¶], Göran Lindbergh[‖], Rakel Wreland Lindström[‖,] and German Salazar-Alvarez[†,§,*]*

[†]Department of Materials and Environmental Chemistry, Arrhenius Laboratory, Stockholm University, SE-10691 Stockholm, Sweden

[§]Wallenberg Wood Science Center (WWSC), Teknikringen 58, SE-100 44, Stockholm, Sweden

[‖]Applied Electrochemistry, Department of Chemical Engineering, KTH Royal Institute of Technology, SE-100 44 Stockholm, Sweden

Additional Experimental details.

AFM Characterization. Figure S1 shows the AFM characterization of the cellulose nanofibers (CNF).

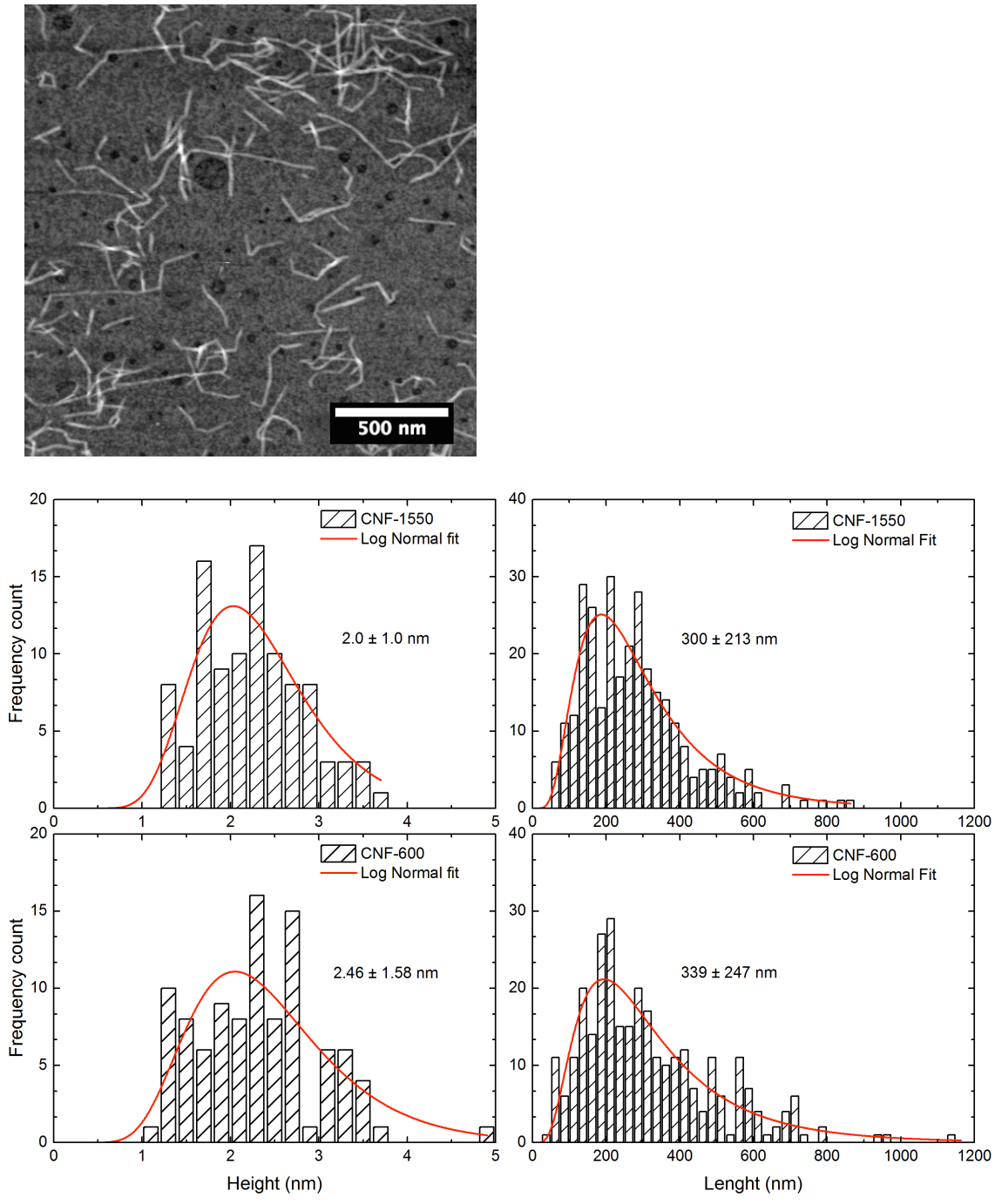

Figure S1 . (A) AFM image of Na-CNF-1550. (B) Length and height distribution of Na-CNF-1550 and Na-CNF-600.

Water uptake of the CNF membrane. Table SI shows the relative water uptake of the CNF films in the carboxylic (H-) and carboxylated (Na-) form exposed at the different relative humidities.

Relative Humidity (%)	H-CNF - 600	H-CNF - 1500	Na-CNF - 600	Na-CNF - 1500
55	7.5 ± 0.4	9.5 ± 1.1	9.4 ± 1.4	10.6 ± 0.3
65	8.3 ± 0.4	10.4 ± 1.0	10.9 ± 1.5	12.5 ± 0.2
75	10.4 ± 0.2	13.4 ± 0.8	13.0 ± 1.4	15.6 ± 0.6
85	13.5 ± 0.4	16.7 ± 1.0	17.7 ± 2.9	25.7 ± 1.9
95	39.5 ± 2.6	45.9 ± 4.9	197.0± 21.5	237.9 ± 45.4

Table SI relative water uptake of the CNF films in the carboxylic (H-) and carboxylated (Na-) form exposed at the different relative humidity values.

Number of water molecules per carboxylic group (λ). The water content, which represents the number of water molecules per carboxylic groups, has been calculated according to by

$$\lambda(RH) = \frac{W_{RH} - W_{dry}}{W_{dry}} \times \frac{EW}{18} \qquad \text{eq. S1}$$

For CNF the value of equivalent molecular weight (EW) in g/mol has been calculated using the surface charge density of the CNF. The values are reported in Figure S2.

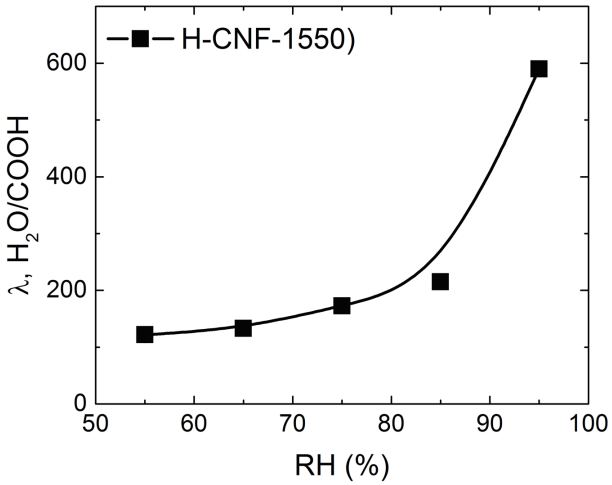

Figure S2 Number of water molecules per carboxylic groups (λ) of the H-CNF-1550

SAXS radial integrated intensity of CNF with Na counter ions. Figure S3 shows the scattering pattern of Na-CNF-1550 and Na-CNF-600.

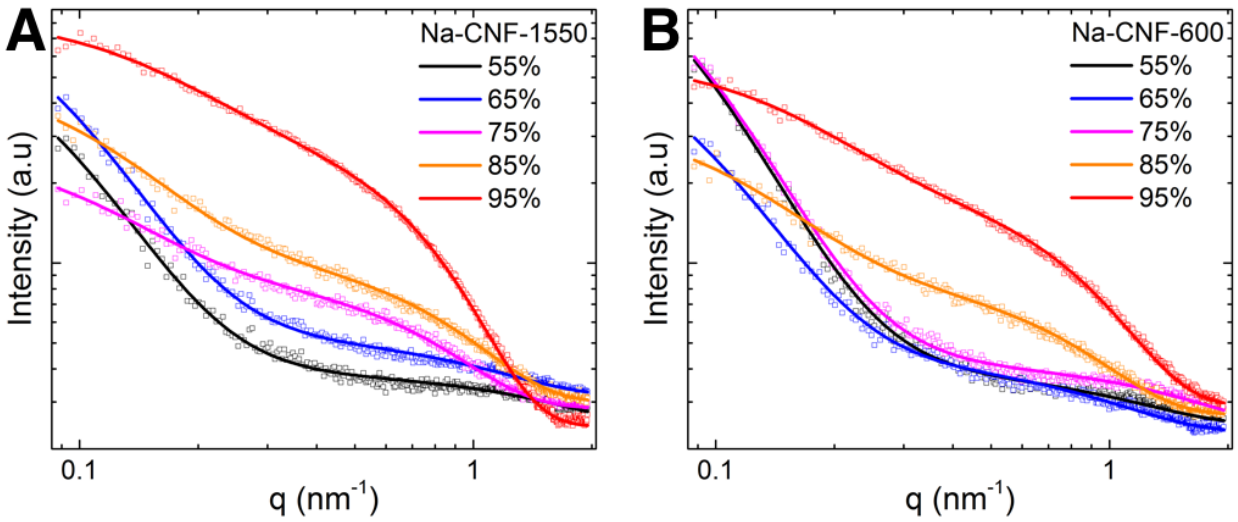

Figure S3: SAXS pattern of Na-CNF membranes as a function of RH.

Proton conductive membranes based on carboxylated cellulose nanofibres and their proton exchange membrane fuel cell performance

Valentina Guccini[†,§,‡], *Annika Carlson*[‖,‡], *Shun Yu*[†,§,¶], *Göran Lindbergh*[‖], *Rakel Wreland Lindström*[‖,*] *and German Salazar-Alvarez*[†,§,*]

[†]Department of Materials and Environmental Chemistry, Arrhenius Laboratory, Stockholm University, SE-10691 Stockholm, Sweden

[§]Wallenberg Wood Science Center (WWSC), Teknikringen 58, SE-100 44, Stockholm, Sweden

[‖]Applied Electrochemistry, Department of Chemical Engineering, KTH Royal Institute of Technology, SE-100 44 Stockholm, Sweden

ABSTRACT

The performance of carboxylated cellulose nanofibers (CNF) membranes has been measured in-situ as a function of CNF surface charge (600 and 1550 μmol g^{-1}), membrane thickness and fuel cell relative humidity (RH 55 to 95 %). The structural evolution of the membrane as a function of RH has been measured by Small Angle X-ray scattering, showing that water channels are formed

above 75 % RH. The amount of absorbed water depends on the membrane surface charge and counter ions (Na^+ or H^+). The high affinity of CNF for water and the high aspect ratio of the nanofibers, together with a well defined and homogenous membrane structure, ensures a proton conductivity exciding 1 mS cm^{-1} at 30 °C between 65 and 95 % RH, around two orders of magnitude larger than previously reported values and only one order of magnitude lower than Nafion 212. Moreover the CNF membranes are characterized by a lower hydrogen crossover than Nafion, despise been ≈ 30 % thinner. Thanks to their environmental compatibility and promising fuel cell performance the CNF membranes should be considered for new generation PEMFCs.

INTRODUCTION

Proton exchange membrane fuel cells (PEMFC) are devices capable of producing electrical power from hydrogen gas. The high specific energy and energy density of hydrogen compared with batteries make PEMFC particularly attractive for propulsion of heavy duty and long distance vechicles.[1] A critical component of the PEMFC is the membrane electrode assembly (MEA), which consists of two electrodes separated by a proton exchange membrane (PEM). The electrodes have a porous structure that allows the mass transport of the reactants and the removal of produced water. The PEMs have to meet the requirements of high proton conductivity and electrical isolation, low fuel and oxidant permeability, low swelling and high stability during operation.[2,3] The most commonly used membrane material is Nafion, a perfluorosulfonic acid polymer develop

from Du Pont in the 1970s. Nafion membranes are characterized by high conductivity (> 100 mS cm^{-1}) which strongly depends on the fuel cell operation parameters.[4,5] Currently it is theorized that the protons are transported through water channels formed as the Nafion polymer orients into hydrophobic and hydrophilic domains. As the water content decreases, the continuity to the hydrophilic domains decreases, thus the ions mobility and the conductivity of Nafion membranes decreases under drier conditions.[5–8]. This has been shown by a linear decrease when the relative humidity (RH) is lowered from 90 and 50 %.[9–13]

The increased demand and interest for cost and environmental effective materials other than Nafion [2,14] have pushed the research efforts to study alternative membranes characterized by a wider range of operation conditions in terms of RH and temperature without sacrificing the performance.

In this regard, thanks to their chemical stability, advantegeous mechanical and optical properties, environmental benignity, availability and versatility in manufactory process,[15,16] the use of cellulose nanomaterials in energy applications such as lithium ion batteries [17–21] and PEMFC itself[22,23] has increased dramatically in recent years.[24–26] All different types of nanocelluloses[15] have been investigated in PEMFCs: bacterial cellulose (BC) membranes have shown a low conductivity, ≈ 0.008 mS cm^{-1} at 40 °C and 98 % RH.[27] Bayer et al. studied carboxylated cellulose nanofibers (CNF) and cellulose nanocrystals (CNC) membranes as PEM for high temperature application and obtained a slightly higher performance characterized by a maximum conductivity value at 100% RH of 0.05 mS cm^{-1} (100 °C) and 0.01 mS cm^{-1} (30 °C) using in an ex-situ measurement replicating the fuel cell environment.[22] Jankowska et al.[23] compared the performance of several nano- and microcelluloses and observed a maximum proton conductivity of ≈ 0.001 mS cm^{-1} at 90 °C under non-controlled RH conditions. The reported values clearly show that the nature

and dimensions of cellulose have a strong impact on the performance. Fine-tuning of the membrane chemistry, structure and macroscopic characteristic can offer an alternative way to improve the performance without compromising the environmental and sustainability benefits of nanocellulose.

In this study, we have evaluated the in-situ fuel cell conductivity of ultrathin CNF possessing different concentrations of surface carboxylate groups casted as membranes of varying thickness. The conductivity as a function of RH was correlated with the membranes water uptake and the evolution of their internal structure was determined using small angle X-ray scattering (SAXS). We found a proton conductivity in excess of 1 mS/cm at 30 °C and between 65 and 95 % RH, i.e., around two orders of magnitude larger than previously reported values, and relatively independent of the humidity values. Our results show that the CNF membranes have the potential to reach a performance close to that of traditional Nafion membranes, making it a promising and relevant candidate for PEM fuel cells.

MATERIAL AND METHODS

CNF preparation. The carboxylated CNF were prepared by TEMPO-mediated oxidation of cellulose pulp, followed by mechanical fibrillation of the oxidized pulp. The never-dried cellulose pulp was supplied by Domsjö Fabriker AB (Domsjö, Sweden). The pulp was washed with a solution of HCl at pH 2, after which it was oxidized following the protocol of Saito et al.[20,28] Typically, 40 g (dry content) of pulp were suspended in 2 L of deionized water and stirred together with the TEMPO catalyst (4 mmol) and sodium bromide (40 mmol) for 1 h. A solution of 0.5 M sodium hydroxide was used to adjust the pH to 10 and to keep it constant during the reaction, while sodium hypochlorite (9 wt% active chlorine) was slowly added. Specifically, 37.5 and 80 mmol

of sodium hypochlorite were added to obtain, respectively, 600 and 1550 μmol g^{-1} of carboxylic groups. After the chemical treatment, the oxidized pulp was washed with deionized water and redispersed with a concentration of 1 wt%. The mechanical fibrillation was performed in two steps with a microfluidizer M-110EH, Microfluidics Corp. Firstly, the pulp was passed 3 times through two chambers with a channel size of 400 and 200 μm at 925 bar, then 9 times through two smaller chambers of 200 and 100 μm at 1600 bar. After the chemical treatment, part of the 1 wt% transparent CNF gel was diluted to 0.3 wt% and sonicated for 8 min with a probe sonicator (20 kHz, 80 % total power, 250 mL max volume). The suspension was centrifuged to remove the impurities after the sonication and the 0.3 wt% CNF suspension was ready to use. Both sonicated and non-sonicated CNF membranes were tested in the in-situ FC.

CNF size and charge determination. The length and height of CNF (see Supporting Figure S1) were determined from the micrographs acquired by atomic force microscopy (Veeco Dimension 3100 SPM) using the tapping mode in air. The samples were prepared by depositing 300 μL of 0.01 wt% suspension onto pre-treated mica substrate with 3-aminopropyl triethoxysilane (Sigma Aldrich, 99 %). The excess of suspension was removed by a stream of air. The surface charge was determined by conductometric titration on the oxidized pulp, following the protocol reported in literature.[20]

Membrane water uptake and ion exchange. The cellulose membranes were ion-exchanged by submerging them in solution of 0.01 M sulfuric acid for 30 min and then rinsed in Milli-Q water until neutral pH. The membranes before the ion exchange are named CNF-COONa, while the ones after the ion exchange are CNF-COOH. The Nafion 212 membrane was used as received. The CNF membranes water uptake was measured at 30 °C and 55, 65, 75, 85 and 95 % RH by

conditioning the membrane for two days in controlled humidity and temperature condition. The increase of weight due to the water absorption was measured with a balance with a 10 μg precision. Each measurement was done on three different replicas. The water uptake was calculated according to the following equation

$$W_{\%}(RH) = \frac{W_{RH} - W_{dry}}{W_{dry}} \times 100 \quad (1)$$

in which W_{RH} is the weight of the membrane at specific RH condition and W_{dry} is the weight of the dry membrane, dried at 105 °C overnight before the measurement.

Membrane casting and characterization. The CNF membranes were casted in Petri dishes with a diameter of 5.5 cm. The appropriate amount of 0.3 wt% CNF suspension was dried at 30 °C and 50 % RH for 3 days. The thickness of the CNF membranes was measured by a High-Accuracy Digimatic Micrometer MDH-25MB (Mitutoyo) with a precision of 0.1 μm. The images of the surface and the cross-section of the membrane were obtained by scanning electrode microscope (SEM) JEOL JSM-7401F.

In-situ FC electrochemical characterization. After the ion exchange the membranes were mounted in a Fuel Cell Technologies cell housing between two 2.5 cm^2 commercial 0.5 mg Pt cm^{-2} on cloth gas diffusion electrodes (Fuel Cells Etc). The cell was transferred to a fuel cell set-up and heated to a cell temperature of 30 °C and 95 % RH under nitrogen flow and left to equilibrate 2 h in order to ensure similar initial conditions for all tests. The experiments were performed as follow: impedance (open-circuit, amplitude 1 mA, 100 kHz–1 Hz, under N_2/N_2 gas), cyclic voltammetry (30 mV s^{-1}, 0.1 V-1.2 V, under N_2/H_2 gas) and Crossover current density measurements (1 mV s^{-1}, OCP-0.7 V, under N_2/H_2 gas) were performed using 60 mL min^{-1} nitrogen

flow and 30 mL min^{-1} hydrogen flow. Thereafter, current-voltage curves were measured from Open Circuit Voltage (OCV) to 0.3 V at a scan rate of 1 mV s^{-1} with 50 mL min^{-1} oxygen gas and 30 mL min^{-1} hydrogen gas on either side of the membrane. The change in conductivity and gas crossover with relative humidity was measured after the sequence above going from high humidity to low with nitrogen gas at the working electrode and hydrogen gas at the counter electrode.

Small Angle X-ray Scattering. The measurements were carried out at the beamline P03 "MiNaXS", of PETRA III storage ring, at the Deutsches Elektronen-Synchrotron (DESY), Germany. The incident X-ray beam had a wavelength of 0.0957 nm and a beam size of about 20×20 μm^2. The sample-to-detector distance was calibrated by dry rat-tail collagen to 2500 ± 0.1 mm . The scattering patterns were recorded using a 2D-pixel detector (Pilatus 1M). The samples were scanned at seven different sample positions and 1D scattering pattern of them ($I(q)$) was extracted via radial integration for minimized beam damage and representative average. The $I(q)$ is normalized to Porod invariant Q to compensate the scattering intensity change due to the volume fraction change and highlight the structure information. $Q = \int_0^\infty q^2 I(q) dq = 2\pi^2 \Delta\rho^2 \varphi(1-\varphi)$, where $\Delta\rho$ is the electron density difference between CNF and water, φ is the volume fraction of CNF. Stripes of the CNF membranes (thickness ≈ 15 μm) were mounted in a conditioned chamber with control humidity and temperature. Each sample has been conditioned for 2 days at each specific humidity (55, 65, 75, 85 and 95 %) and sealed. Previous to the measurement the membrane was conditioned inside the chamber for 15 min. The acquisition time for each measurement was 0.5 s for the membrane conditioned at 95 and 85 % RH and 1 s for the other conditions. The acquisition times were selected after comparing the intensity and the scattering profile changes under continuous X-ray beam exposure.

RESULTS

The CNF membranes were manufactured from aqueous suspension of nanofibers characterized by high aspect ratio with a length of ≈ 300 nm and height of ≈ 2 nm (see Supporting Figure S1). The CNF membranes, consisting of nanofibers with a surface charge of 600 and 1550 μmol g^{-1} (respectively CNF-600 and CNF-1550), were compared with respect to water uptake and conductivity. Figure 1A shows the water uptake of the CNF-600 and CNF-1500 membranes at different RH (55-95 %) before and after being ion-exchanged (see also Table S1 supporting information).

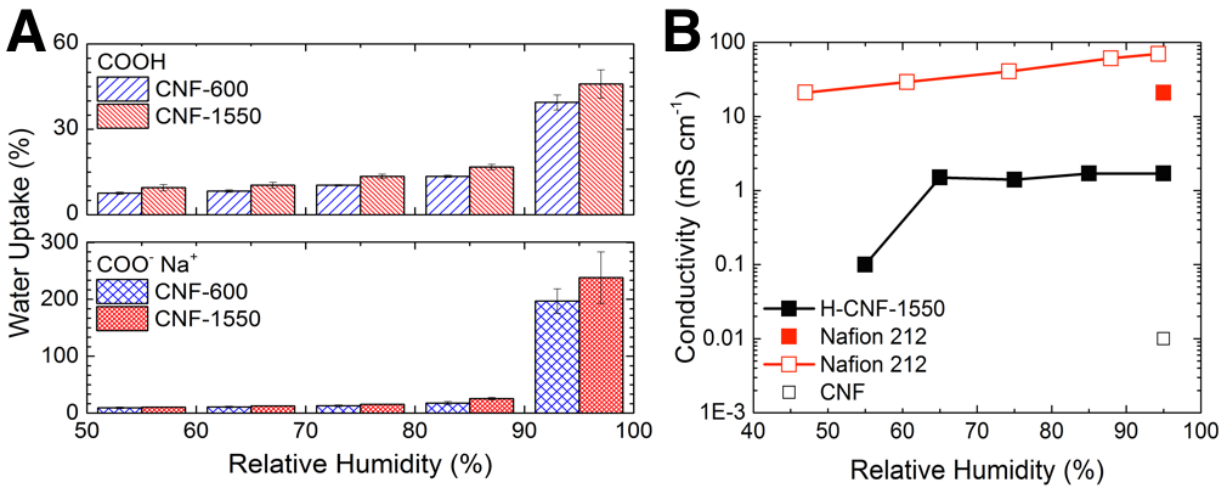

Figure 1. (A) Water uptake of carboxylated (COONa) and carboxylic (COOH) CNF membrane. (B) Experimental conductivity of the H-CNF-1550 membrane in this work, Nafion 212,[12] and CNF.[22]

The water uptake for the CNF-COOH increases about one order of magnitude from 55 to 95 % RH, while for the CNF-COONa ones increases two orders of magnitude. At 95 % RH the water uptake of CNF-COONa is much higher than the CNF-COOH, approximately 500 % bigger. The

CNF membrane with higher surface charge (1550 μmol g^{-1}) have higher water uptake compared to the ones with lower (600 μmol g^{-1}), as reported elsewhere.[16,28] The carboxylic groups have a lower hydration shell than the carboxylated groups reducing the water uptake, which translate in lower swelling and thus higher dimensional stability. Moreover in CNF-COOH the interaction between cellulose nanofibers is higher due to the hydrogen bond, which results in a higher Young's modulus.[29]

The in-situ conductivity of H-CNF-1550 was measured as a function of RH, from 95 to 55 % and the results are shown in Figure 1B. At 95 % RH, the conductivity is close to 2 mS cm^{-1}, two orders of magnitude higher than previously reported values for nanocellulose-based membranes.[22] However, the conductivity of H-CNF-1550 membranes is still 10-50 times lower than that of Nafion 212 both in control experiments and literature data[10]. The deviation from literature data for Nafion is most likely related to MEA preparation and internal resistances within the cell housing, however, the experimentally measured value can be directly compared to the CNF. The conductivity of H-CNF-1550 is constant above 65 %, but drops significantly at 55 % RH, whereas the conductivity of Nafion decreases almost logarithmically with decreasing RH.

These measurements suggest that in-situ conductivity of CNF membranes is less sensitive to humidity changes than Nafion, probably due to the higher hydrophilic character and the different water interaction of CNF compared to Nafion. The number of water molecules per proton conductive site of CNF (Figure S2 supporting information), represented by the water content λ,[30,31] is more than 100 times higher than that of Nafion 212.[10]

The CNF membrane conductivity was also measured for different thickness and surface charges, Table 1 summarizes the conductivity of the H-CNF-1550 and H-CNF-600 obtained by electrochemical impedance spectroscopy (EIS) in the fuel cell.

	Conductivity (mS cm^{-1})	
Sample Name	Thickness ca. 14 µm	Thickness ca. 24 µm
H-CNF-600	1.4± 0.1	1.2 ± 0.4
H-CNF-1550	1.5 ± 0.2	1.4 ± 0.2

Table 1. Conductivity of H-CNF membranes as a function of thickness, measured under N_2/N_2 gas.

The conductivity of the H-CNF-1550 14 µm is the highest among the CNF membranes and generally all the CNF membranes are characterized by a value only one order of magnitude lower than Nafion 212 (≈ 20 mS cm^{-1}), when measured under the same conditions. The conductivity is observed to be independent of the membranes thickness, indicating that the membranes have a homogenous charge distribution. The difference between H-CNF-1550 and H-CNF-600 is given by the differences in surface charge of the two samples, whereas the difference between CNF and Nafion can have the following explanations. First, the pKa of Nafion is around -6 while the carboxylic acid present on the CNF surface is ≈ 3-4, thus it is significantly less acidic. Second, Nafion is characterized by the presence of hydrophobic and hydrophilic domains, that have been proven to enhance the proton conductivity, by the formation of confined water micro-channels in the Nafion membrane.[11]

In order to improve the understanding of how the CNF membrane structure affects the conductivity, the membranes were characterized using electron microscopy and small angle X-ray scattering (SAXS). The membranes consist of layers where the CNF forms an entangled network.[32] Figure 2A and 2B show the surface and the cross-section of the H-CNF-1500 membrane. At the surface, the nanofibers are randomly oriented in the plane and along the cross-section they are arranged together in layers. This layered structure is characteristic of CNF films dried by slow

evaporation of the solvent[33,34] and which gives the film barrier properties against gases such as oxygen and hydrogen.[35] Thanks to the controlled slow drying, the dried CNF films are dense and transparent. The evolution of CNF membrane structure upon water absorption at increasing RH was studied by SAXS and it shown in Figure 2C and 2D.

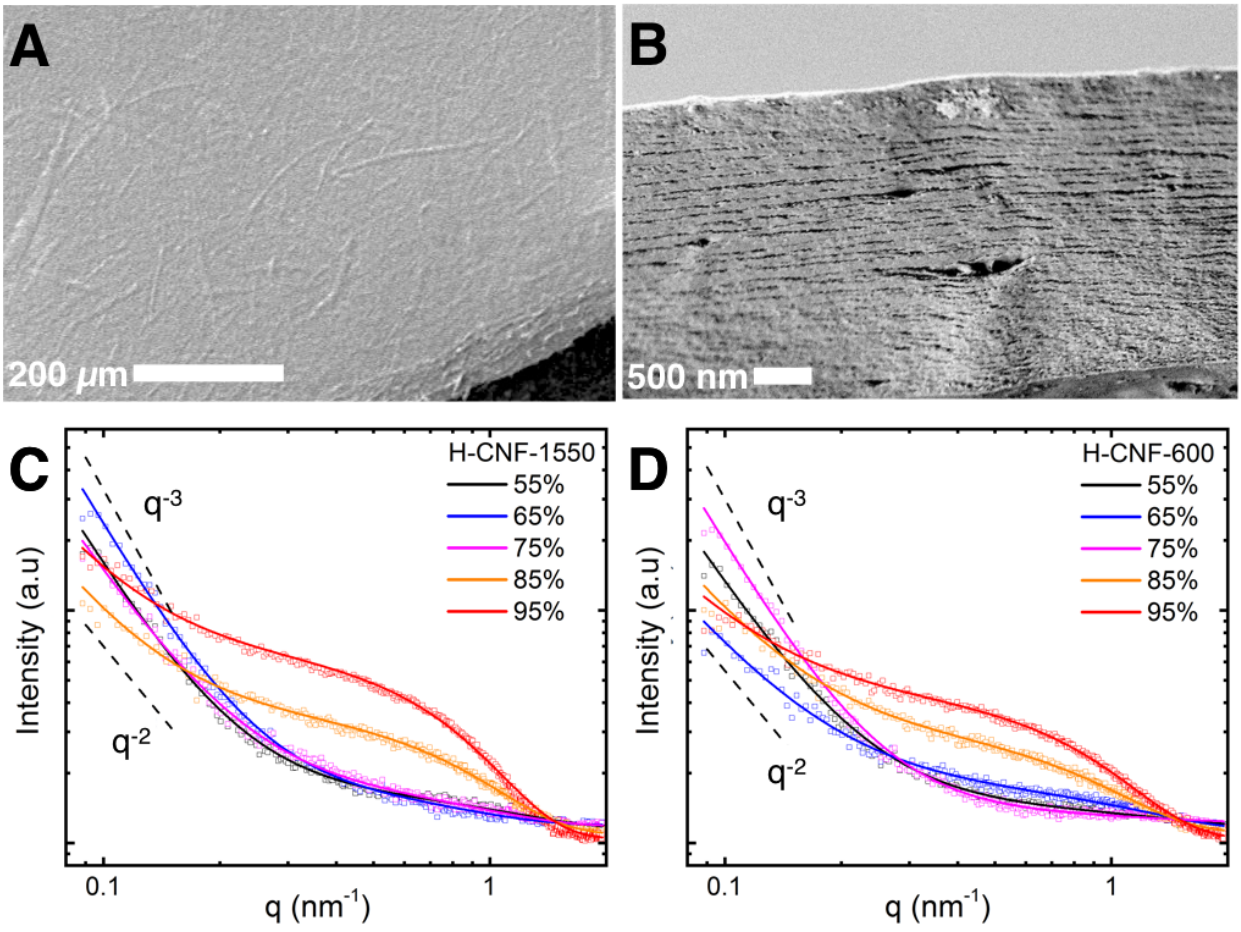

Figure 2. (A) SEM image of H-CNF-1500 membrane and (B) its cross-section. (C) Radial integrated intensity of SAXS pattern of H-CNF-1550 and (D) H-CNF-600 as a function of relative humidity (55-95 %).

The SAXS data were fitted using two-stage model written as:

$$I(q) = \frac{A}{q^n} + B \cdot \exp\left(-\frac{q^2 \cdot \Xi^2}{2}\right) + C \qquad (2)$$

where A and B are scaling factors and C is a constant background. The first term to the right is a power law function depicting the large structure in scaling exponent n, known as Porod exponent, which is related to the complexity of the network connection. As n decreases when the RH increases, it suggests that in the tested RH condition, the CNF agglomerates are kept highly entangled, despite water swelling the nanofiber network. Generally, an exponent $1< n <3$, it indicates that the network may adopt a bulk fractal dimension, whereas $2 < n <3$, it is known as mass fractal, which is observed in most of cases in this study (see support information Table S2). The second term adopts the form of a Gaussian function, which is known for describing an average size Ξ of small features. In this case, it is related to the pores embedded in the densely packed CNF membranes. Ξ accounts for the distinct feature that appears around $q \approx 0.59$ nm^{-1}, that increases with the water content and it is attributed to the formation of water channels in those pores. Indeed, due to the swelling induced by the water uptake the size of the pores increases from ≈ 1.0 nm at 55-75 % to ≈ 2 nm at 95 % RH (See support information Table S2), slightly smaller than the average diameter of CNF. This observation is in line with the water uptake data presented in Figure 1A. At 95 % RH the CNF membrane have a pore size comparable with fully hydrated Nafion with width of 2.5 ± 0.2 nm using electron microscope cryotomography. [36] An increase of porosity during the swelling increases the scattering volume (CNF-pore), despite the incorporation of water condensing in the membrane channels reduces the scattering contrast (CNF-water interphase), leading to the increase in intensity at the high q range. The higher scattering intensity of H-CNF-1500 (Figure 2C) is associated with a higher water uptake compare to H-CNF-600 (Figure 2D), as the amount of water depends on the type of counter ions (Na^+ or H^+) and on the amount of surface charge on the nanofibers (Figure 1A). The SAXS pattern of the Na-CNF-1550 and Na-CNF-600 (Figure S3 and Table S2 supporting information) shows higher intensity and a

242 less define feature at high q, due to the higher amount of water and higher swelling. The interaction
243 between water and cellulose has been extensively studied,[37–39] showing that the water is present in
244 the CNF as absorbed and bound water. The movable bound water is located between the nanofiber
245 agglomerate-agglomerate interface whereas the immobile portion is between nanofibers belonging
246 to the same agglomerate.[39] The absorbed water promotes the formation of channels with increase
247 humidity (feature at high q). Intuitively, the mobility of the absorbed water is higher than the bound
248 water, suggesting that the predominant and most favorable proton conduction mechanism in CNF
249 membrane may occur via the hydrogen bonds present in the liquid water (Grotthuss mechanism).
250 The structure evolution of the membrane as a function of humidity suggests that the formation of
251 the water channels in the structure mainly form above 75 % RH. At the same time the in-situ
252 conductivity remains constant towards 65% RH (figure 1B) despite the structural changes and the
253 variation in water content (Figure 1A), meaning that bound water has to contribute to the proton
254 conduction. Indeed, the difference on the amount of absorbed water between 55 and 65 % RH for
255 the H-CNF-1550 is only around 1 %. Thus, the bound water may be able to ensure similar proton
256 conduction at 55 % RH and the drop in conductivity (Figure 1B) it may due to some fuel cell
257 operational causes. The fact that the value of in-situ conductivity vs RH is constant, it is
258 unprecedented for nanocellulose based membranes. Bayer at al. show that ex-situ proton
259 conductivity decreases approximately 2 orders of magnitude between 80 and 70 % RH.[22] The
260 lower conductivity towards low RH could be attributed to the use of thick CNF with a fiber
261 thickness of tens to hundreds nanometers, *cf*. the CNF used in this study with a thickness of ≈ 2
262 nm (Figure S1 supporting information). This likely leads to a decreased amount of surface water
263 in the membrane. Recently, Jankowska et al. showed that films made of nanocellulose had higher
264 proton conductivity compared to the ones made of larger microcellulose,[23] supporting our results

that highlight the importance of high aspect ratio nanofibers and well defined and homogenous membrane structures (achievable by controlled slow drying conditions), which are tightly connected with the membrane water interaction and thus with the proton conductivity.

In addition to high proton conductivity barrier properties towards H_2 and O_2 is another key factor for a well-functioning PEM, which has been previously shown for CNF.[35]

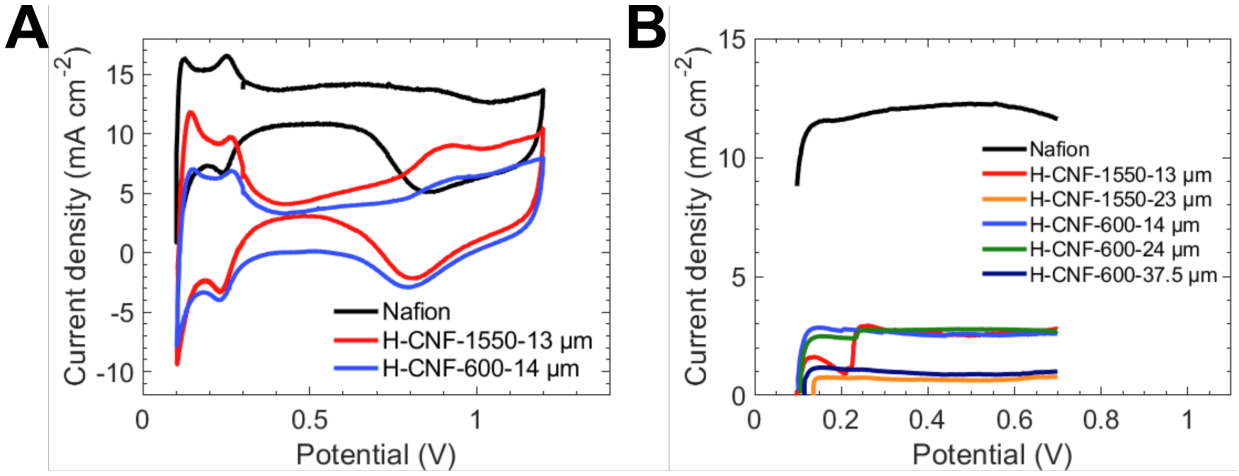

Figure 3. Hydrogen cross-over characterization of CNF membranes compared to Nafion 212. (A) Cyclic Voltamogram of the CNF membrane as a function of surface charge density. (B) Hydrogen cross-over current density of the CNF membranes as a function of surface charge and thickness.

Here the in-situ characterization of the H_2 permeability, were performed using cyclic voltammetry (CV) and crossover current density measurements. Figure 3A shows the cyclic voltammograms of the H-CNF membranes with 600 and 1550 µmol g^{-1} and Nafion 212. Both CNF and Nafion curves show similar size of the adsorption and desorption peaks for hydrogen onto the 100 and 110 facets of the Pt catalyst (peaks below 0.4 V). This indicates that the electrodes in all tests have similar amounts of catalytic sites available and that the use of CNF membranes does not affect the catalyst layer. At N_2 /100 % H_2 conditions in a fuel cell the crossover of hydrogen from the counter/reference electrode results in a typical lift of the CV for Nafion. However, both H-CNF

membranes curves center around a lower current density than Nafion, which is an indication of a lower hydrogen crossover at these operating conditions, despite the CNF membranes being are significantly thinner (≈ 14 μm compared to 51 μm). The low hydrogen permeability is probably related to the layered structure and high density of the CNF membranes (Figure 2A and 2B). The same conclusions were reached for CNF and CNC membrane prepared by vacuum filtration and hot pressing.[22] The cross-over current density (Figure 3B), proportional to the hydrogen cross-over, confirms the observations in the CV characterization. Nafion is characterized by the highest cross-over current density and among the H-CNF membranes the H-CNF-600 has the lowest cross-over. No significant difference between H-CNF-600 and H-CNF-1550 is observed, but a small decrease can be seen with increased membrane thickness. Calculating the permeability coefficients for the CNF membranes gives $1.5\pm0.5\times10^{-11}$ and $2\pm0.5\times10^{-11}$ mol cm^{-1} s^{-1} bar^{-1} for the thicker and thinner membranes respectively. The values are very close and indicate that the permeability is not changed by altering the thickness. For Nafion the corresponding value in our setup and cell housing is an order of magnitude higher, i.e., 3.1×10^{-10} mol cm^{-1} s^{-1} bar^{-1}.

The fuel cell performance of the investigated membranes is shown in Figure 4. The influence of the CNF surface charge and thickness of membranes on performance was evaluated by current density–voltage measurements in a fuel cell during operation at 30 °C and 95 % RH. The IR-corrected (dashed lines) and non-corrected (solid lines) polarization curves of H-CNF-1550 and H-CNF-600 membranes at different thickness are shown. The IR-corrected lines are compensated using the high frequency resistance, from which the conductivity was calculated, and removes any differences in resistance due to various thickness of the membranes and any other resistive losses in the cell.

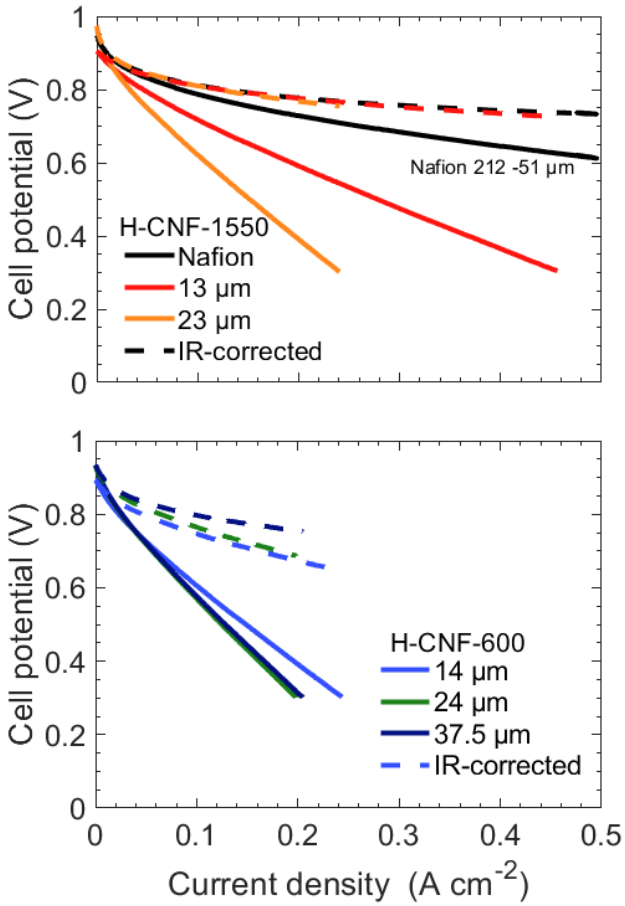

304

305 **Figure 3.** Polarization curves of CNF membranes as a function of surface charge and thickness.
306 caption polarization, as well Nafion 212. The dashed curves represent IR-corrected measurements.

307 All the CNF membranes have a high open circuit voltage, close to that of Nafion, which is
308 expected from the low hydrogen crossover. In the current voltage measurements, the H-CNF-1550
309 membranes show a superior performance to H-CNF-600, although still having a higher resistance
310 than Nafion. These results are in accordance with the conductivity measurements above. The
311 higher performances of the H-CNF-1550 membranes compared to the H-CNF-600 is the result of
312 the higher amount of surface charge, which leads to a higher conductivity. The increased water
313 content and the more pronounced formation of water channels, observed by SAXS measurements,
314 for higher charge should also facilitate the ionic transport. The lower conductivity and so, lower

315 performance compared to Nafion may be related to the lower acidity of the carboxylic groups,
316 interfacial resistance between electrode and membrane, and/or differences in membrane structure.
317 However, the good cross-over properties of very thin CNF membranes show promise to reduce
318 the internal resistance of the fuel cell in future studies of MEA preparation. Further, as the CNF
319 films are characterized by better mechanical properties than Nafion, they could provide a robust
320 alternative in several energy applications. For example Nafion 117 at 30 % RH have Young's
321 modulus of ≈ 200 MPa,[40] whereas Na-CNF films of ≈ 15 GPa.[29] However, for both CNF and
322 Nafion films the Young's modulus decreases with an increased relative humidity. Thereby, these
323 materials are very promising for PEMFC applications, but further optimization of the MEA under
324 varying fuel cell operating conditions is required.

325 In conclusion, the water uptake of the CNF membrane depends on the amount of surface charge
326 and its counter ions. The high affinity of CNF for water ensures stable proton conductivity despite
327 the variation of RH. Indeed, the number of water molecules per proton conductive site is more
328 than 100 times higher than that for Nafion 212. Our experiments suggest that the bound water on
329 the nanofiber agglomerate–agglomerate interfaces has a key role in ensure the proton conduction
330 independently to the amount of absorbed water and gives a dominant contribution specially at low
331 RH. The structural changes with varying humidity observed with SAXS show that water channels
332 are formed only above 75 % RH. Our results highlight the importance of CNF with high aspect
333 ratio and a well-defined and homogenous membrane structure (achievable by controlled slow
334 drying conditions) in order to improve the performance of CNF based PEM. All the membranes
335 are characterized by a proton conductivity only one order of magnitude lower than Nafion 212.
336 The conductivity of the CNF-membranes was shown to depend on surface charge and among them
337 the H-CNF-1550 (14 μm thickness) has the highest conductivity and performance. Further, the

CNF membranes are characterized by lower hydrogen crossover then Nafion despite being thinner. Thanks to the superior mechanical properties of CNF membranes compared to Nafion, they can be fabricated to be thinner, potentially reducing the internal cell resistance, without compromising the gas barrier properties. Lastly, our study shows that CNF membranes with their environmental compatibility, low gas crossover and promising fuel cell performance should be considered for use in a new generation PEMFCs.

ASSOCIATED CONTENT

Supporting Information. The Supporting Information is available free of charge on the ACS Publications website. It contains details on morphological characterization, additional data on the water uptake and SAXS characterization of the membrane. (file type PDF)

AUTHOR INFORMATION

Corresponding Authors

*Email: Rakel Wreland Lindström (rakel2@kth.se)

German Salazar-Alvarez (gersal@protonmail.com)

Present Address

¶ RISE Research Institutes of Sweden, Lund, Sweden

Author Contributions

The manuscript was written through contributions of all authors. All authors have given approval to the final version of the manuscript.

‡Valentina Guccini and Annika Carlson contributed equally.

ACKNOWLEDGMENT

The authors thank Sugam Kumar, Luis Valencia, Aji P. Mathew and Peng Liu for the experimental support during the beam time. The Knut and Alice Wallenberg foundation is acknowledged for the financial support through the Wallenberg Wood Science Center. The research was also partially sponsored by the Swedish Vehicle Research and Innovation program, the Swedish Energy Agency and the Swedish governmental initiative StandUp for Energy. SY thanks the financial support from the Swedish Research Council VR (Grant 2016-06959). We acknowledge DESY (Hamburg, Germany), a member of the Helmholtz Association HGF, for the provision of experimental facilities. Parts of this research were carried out at PETRA III and we would like to thank Wiebke Ohm for assistance in using the beamline P03. This work benefited from the use of the SasView application, originally developed under NSF award DMR-0520547. SasView contains code developed with funding from the European Union's Horizon 2020 research and innovation programme under the SINE2020 project, grant agreement No 654000.

REFERENCES

(1) Cano, Z. P.; Banham, D.; Ye, S.; Hintennach, A.; Lu, J.; Fowler, M.; Chen, Z. Batteries and fuel cells for emerging electric vehicle markets. Nat. Energy 2018, 3 (4), 279–289.

(2) Steel, B.; Heinzel, A. Materials for Fuel Cell Technologies. Nature 2001, 414, 345–352.

(3) Wang, Y.; Chen, K. S.; Mishler, J.; Cho, S. C.; Adroher, X. C. A review of polymer electrolyte membrane fuel cells: Technology, applications, and needs on fundamental research. Applied Energy. 2011, pp 981–1007.

(4) Smitha, B.; Sridhar, S.; Khan, A. A. Solid polymer electrolyte membranes for fuel cell applications - A review. J. Memb. Sci. 2005, 259 (1–2), 10–26.

(5) Mauritz, K. A.; Moore, R. B. State of Understanding of Nafion. Chem. Rev. 2004, 104 (10), 4535–4586.

(6) Savadogo, O. Emerging membranes for electrochemical systems: Part II. High temperature composite membranes for polymer electrolyte fuel cell (PEFC) applications. J. Power Sources 2004, 127 (1–2), 135–161.

(7) Bose, S.; Kuila, T.; Nguyen, T. X. H.; Kim, N. H.; Lau, K. T.; Lee, J. H. Polymer membranes for high temperature proton exchange membrane fuel cell: Recent advances and challenges. Prog. Polym. Sci. 2011, 36 (6), 813–843.

(8) Rosli, R. E.; Sulong, A. B.; Daud, W. R. W.; Zulkifley, M. A.; Husaini, T.; Rosli, M. I.; Majlan, E. H.; Haque, M. A. A review of high-temperature proton exchange membrane fuel cell (HT-PEMFC) system. Int. J. Hydrogen Energy 2017, 42 (14), 9293–9314.

(9) Schalenbach, M.; Lueke, W.; Lehnert, W.; Stolten, D. The influence of water channel geometry and proton mobility on the conductivity of Nafion®. Electrochim. Acta 2016, 214, 362–369.

(10) He, Q.; Kusoglu, A.; Lucas, I. T.; Clark, K.; Weber, A. Z.; Kostecki, R. Correlating humidity-dependent ionically conductive surface area with transport phenomena in proton-exchange membranes. J. Phys. Chem. B 2011, 115 (40), 11650–11657.

(11) Einsla, M. L.; Kim, Y. S.; Hawley, M.; Lee, H. S.; McGrath, J. E.; Liu, B.; Guiver, M. D.; Pivovar, B. S. Toward improved conductivity of sulfonated aromatic proton exchange membranes at low relative humidity. Chem. Mater. 2008, 20 (17), 5636–5642.

(12) Anantaraman, A. V.; Gardner, C. L. Studies on ion-exchange membranes. Part 1. Effect of humidity on the conductivity of nafion®. J. Electroanal. Chem. 1996, 414 (2), 115–120.

(13) Zhang, J.; Tang, Y.; Song, C.; Xia, Z.; Li, H.; Wang, H.; Zhang, J. PEM fuel cell relative humidity (RH) and its effect on performance at high temperatures. Electrochim. Acta 2008, 53 (16), 5315–5321.

(14) Yee, R. S. L.; Rozendal, R. A.; Zhang, K.; Ladewig, B. P. Cost effective cation exchange membranes: A review. Chem. Eng. Res. Des. 2012, 90 (7), 950–959.

(15) Klemm, D.; Kramer, F.; Moritz, S.; Lindström, T.; Ankerfors, M.; Gray, D.; Dorris, A. Nanocelluloses: a new family of nature-based materials. Angew. Chem. Int. Ed. Engl. 2011, 50 (24), 5438–5466.

(16) Moon, R. J.; Martini, A.; Nairn, J.; Simonsen, J.; Youngblood, J. Cellulose nanomaterials review: structure, properties and nanocomposites. Chem. Soc. Rev. 2011, 40 (7), 3941–3994.

(17) Leijonmarck, S.; Cornell, A.; Lindbergh, G.; Wågberg, L. Flexible nano-paper-based positive electrodes for Li-ion batteries-Preparation process and properties. Nano Energy 2013, 2 (5), 794–800.

(18) Leijonmarck, S.; Cornell, A.; Lindbergh, G.; Wågberg, L. Single-paper flexible Li-ion battery cells through a paper-making process based on nano-fibrillated cellulose. J. Mater. Chem. A 2013, 1 (15), 4671.

(19) Lu, H.; Behm, M.; Leijonmarck, S.; Lindbergh, G.; Cornell, A. Flexible Paper Electrodes for Li-Ion Batteries Using Low Amount of TEMPO-Oxidized Cellulose Nanofibrils as Binder. ACS Appl. Mater. Interfaces 2016, 8 (28), 18097–18106.

(20) Lu, H.; Guccini, V.; Kim, H.; Salazar-Alvarez, G.; Lindbergh, G.; Cornell, A. Effects of Different Manufacturing Processes on TEMPO-Oxidized Carboxylated Cellulose Nanofiber Performance as Binder for Flexible Lithium-Ion Batteries. ACS Appl. Mater. Interfaces 2017, 9 (43), 37712–37720.

(21) Kim, H.; Guccini, V.; Lu, H.; Salazar-Alvarez, G.; Lindbergh, G.; Cornell, A. Lithium ion battery separators based on carboxylated cellulose nanofibers from wood. ACS Appl. Energy Mater. 2018, acsaem.8b01797.

(22) Bayer, T.; Cunning, B. V.; Selyanchyn, R.; Nishihara, M.; Fujikawa, S.; Sasaki, K.; Lyth, S. M. High Temperature Proton Conduction in Nanocellulose Membranes: Paper Fuel Cells. Chem. Mater. 2016, 28 (13), 4805–4814.

(23) Jankowska, I.; Pankiewicz, R.; Pogorzelec-Glaser, K.; Ławniczak, P.; Łapiński, A.; Tritt-Goc, J. Comparison of structural, thermal and proton conductivity properties of micro- and nanocelluloses. Carbohydr. Polym. 2018, 200, 536–542.

(24) Wicklein, B.; Salazar-Alvarez, G. Functional hybrids based on biogenic nanofibrils and inorganic nanomaterials. J. Mater. Chem. A 2013, 1 (18), 5469.

(25) Muhd Julkapli, N.; Bagheri, S. Nanocellulose as a green and sustainable emerging material in energy applications: a review. Polym. Adv. Technol. 2017, 28 (12), 1583–1594.

(26) Chen, W.; Yu, H.; Lee, S. Y.; Wei, T.; Li, J.; Fan, Z. Nanocellulose: A promising nanomaterial for advanced electrochemical energy storage. Chem. Soc. Rev. 2018, 47 (8), 2837–2872.

(27) Gadim, T. D. O.; Loureiro, F. J. A.; Vilela, C.; Rosero-Navarro, N.; Silvestre, A. J. D.; Freire, C. S. R.; Figueiredo, F. M. L. Protonic conductivity and fuel cell tests of nanocomposite membranes based on bacterial cellulose. Electrochim. Acta 2017, 233, 52–61.

(28) Isogai, A.; Saito, T.; Fukuzumi, H. TEMPO-oxidized cellulose nanofibers. Nanoscale 2011, 3 (1), 71–85.

(29) Benítez, A.; Torres-Rendon, J.; Mikko Poutanen; Walther, A. Humidity and Multiscale Structure Govern Mechanical Properties and Deformation Modes in Films of Native Cellulose Nanofibrils. Biomacromolecules 2013, 14, 4497–4506.

(30) Zawodzinski, T. A.; Gottesfeld, S.; Shoichet, S.; McCarthy, T. J. The contact angle between water and the surface of perfluorosulphonic acid membranes. J. Appl. Electrochem. 1993, 23 (1), 86–88.

(31) Zawodzinski, T. A.; Davey, J.; Valerio, J.; Gottesfeld, S. The water content dependence of electro-osmotic drag in proton-conducting polymer electrolytes. Electrochim. Acta 1995, 40 (3), 297–302.

(32) Guccini, V.; Yu, S.; Agthe, M.; Gordeyeva, K.; Trushkina, Y.; Fall, A. B.; Schütz, C.; Salazar-Alvarez, G. Inducing Nematic Ordering of Cellulose Nanofibers using Osmotic Dehydration. Nanoscale 2018.

(33) Nogi, M.; Iwamoto, S.; Nakagaito, A. N.; Yano, H. Optically Transparent Nanofiber Paper. Adv. Mater. 2009, 21 (16), 1595–1598.

(34) Zhao, M.; Ansari, F.; Takeuchi, M.; Shimizu, M.; Saito, T.; Berglund, L. A.; Isogai, A. Nematic structuring of transparent and multifunctional nanocellulose papers. Nanoscale Horizons 2018, 3 (1), 28–34.

(35) Fukuzumi, H.; Saito, T.; Iwamoto, S.; Kumamoto, Y.; Ohdaira, T.; Suzuki, R.; Isogai, A. Pore size determination of TEMPO-oxidized cellulose nanofibril films by positron annihilation lifetime spectroscopy. Biomacromolecules 2011, 12 (11), 4057–4062.

(36) Allen, F. I.; Comolli, L. R.; Kusoglu, A.; Modestino, M. A.; Minor, A. M.; Weber, A. Z. Morphology of Hydrated As-Cast Na fi on Revealed through Cryo Electron Tomography. 2015.

(37) Berthold, J.; Desbrières, J.; Rinaudo, M.; Salmén, L. Types of adsorbed water in relation to the ionic groups and their counter-ions for some cellulose derivatives. Polymer 1994, 35 (26), 5729–5736.

(38) O'Neill, H.; Pingali, S. V.; Petridis, L.; He, J.; Mamontov, E.; Hong, L.; Urban, V.; Evans, B.; Langan, P.; Smith, J. C.; et al. Dynamics of water bound to crystalline cellulose. Sci. Rep. 2017, 7 (1), 11840.

(39) Lindh, E. L.; Terenzi, C.; Salmén, L.; Furó, I. Water in cellulose: Evidence and identification of immobile and mobile adsorbed phases by2H MAS NMR. Phys. Chem. Chem. Phys. 2017, 19 (6), 4360–4369.

(40) Tang, Y.; Karlsson, A. M.; Santare, M. H.; Gilbert, M.; Cleghorn, S.; Johnson, W. B. An experimental investigation of humidity and temperature effects on the mechanical properties of perfluorosulfonic acid membrane. Mater. Sci. Eng. A 2006, 425 (1–2), 297–304.